Supporting Information

Engineering DNA-Functionalized Nanostructures to Bind Nucleic Acid Targets Heteromultivalently with Enhanced Avidity

Brendan R. Deal, Rong Ma, Victor Pui-Yan Ma, Hanquan Su, James T. Kindt, and Khalid Salaita

Department of Chemistry, Emory University, Atlanta, Georgia 30322, United States

Table of Contents

Materials and Methods

1. Materials

1.1. Oligonucleotides

All oligonucleotides were custom synthesized by Integrated DNA Technologies (Coralville, IA). The table below includes the names and sequences for all oligonucleotides used in this work. Structures of the modifications are shown in Figure S5. Note that segment 6 has an 11T spacer instead of 10T. However, we do not expect that this will impact any findings from this work.

Name	Sequence (5' to 3')
segment 1	/5ThioMC6-D/TTTTTTTTTTACTCTACCACATATA
segment 2	/5ThioMC6-D/TTTTTTTTTTTCCTTGGGAACC
segment 3	/5ThioMC6-D/TTTTTTTTTTGACAGTAAATGCG
segment 4	/5ThioMC6-D/TTTTTTTTTTCAGCAAATGCCA
segment 5	/5ThioMC6-D/TTTTTTTTTTAGGTCATGAATATAA
segment 6	/5ThioMC6-D/TTTTTTTTTTTACAGCAAATATCCT
amine-labeled target	AGGATATTTGCTGTCTTTATATTCATGACCT ACTGGCATTTGCTGAACGCATTTACTGTC ACGGTTCCCAAGGACCTATATGTGGTAGAGT/3AmMO/
amine-labeled target-no spacers	AGGATATTTGCTGTTTATATTCATGACCT TGGCATTTGCTGCGCATTTACTGTC GGTTCCCAAGGATATATGTGGTAGAGT/3AmMO/
patterned template	AGGATATTTGCTGTTTATATTCATGACCT TGGCATTTGCTGCGCATTTACTGTC GGTTCCCAAGGATATATGTGGTAGAGT
mispatterned template	TGGCATTTGCTGAGGATATTTGCTGT GGTTCCCAAGGATTATATTCATGACCT TATATGTGGTAGAGTCGCATTTACTGTC
FAM-labeled target	AGGATATTTGCTGTCTTTATATTCATGACCT ACTGGCATTTGCTGAACGCATTTACTGTC ACGGTTCCCAAGGACCTATATGTGGTAGAGT/36-FAM/
FAM-labeled target-no spacers	AGGATATTTGCTGTTTATATTCATGACCT TGGCATTTGCTGCGCATTTACTGTC GGTTCCCAAGGATATATGTGGTAGAGT/36-FAM/
T10	/5ThioMC6-D/TTTTTTTTTT

1.2. Reagents

Nitric acid (Cat# BDH3044500MLPC) was purchased from VWR (Radnor, PA). Hydrochloric acid (Cat# HX0603-3), sodium phosphate monobasic monohydrate (Cat# SX0710), sodium chloride (Cat# SX0420, GR ACS), potassium chloride (Cat# 1049360500), monopotassium phosphate (Cat# PX1565-1), and Dri-solv methylsulfoxide (Cat# MX1457-7) were purchased from EMD Millipore (Burlington, MA). Gold (III) chloride trihydrate (Cat# 520918-1G), sodium citrate tribasic dihydrate (Cat# S4641-25G), dithiothreitol (DTT) (Cat# 10197777001), sodium dodecyl sulfate (SDS) (Cat# L3771), 3-hydroxypicolinic acid (3-HPA) (Cat# 56197), potassium cyanide (Cat# 60178), potassium hydroxide (Cat# 221473), sodium bicarbonate (Cat# S6014), acetonitrile (Cat# 34998), and tetramethylethylenediamine (TEMED) (Cat# T9281) were purchased from Sigma-Aldrich (St. Louis, MO). Sodium phosphate dibasic was purchased from (Cat# 470302-660) Ward's Science (Rochester, NY). 20x TE buffer (Cat# 42020325-2) was purchased from bioWORLD (Dublin, OH). Quant-IT Oligreen ssDNA reagent (Cat# O7582), Tween20 (Cat# BP337), 6x DNA loading dye (Cat# R0611), ammonium persulfate (APS) (Cat# BP179-25), and SYBR Gold nucleic acid gel stain (Cat# S11494) were purchased from Thermo Fisher Scientific (Waltham, MA). Saline sodium citrate (SSC) buffer (Cat# AM9763) was purchased from Ambion (Austin, TX). Cyanine 5 NHS ester (Cat# 23020) was purchased from Lumiprobe (Hunt Valley, MD). Triethylammonium acetate (Cat# 60-4110-57) and trifluoroacetic acid (Cat# 60-4040-57) were purchased from Glen Research (Sterling, VA). Ammonium citrate (Cat# 09831) was purchased from Fluka Analytical (Charlotte, NC). Tris(2-carboxyethyl)phosphine hydrochloride (TCEP) (Cat# T1656) was purchased from Tokyo Chemical Industry (Tokyo, Japan). 30% Acrylamide/Bis Solution 29:1 (Cat# 1610156) was purchased from Bio-Rad (Hercules, CA).

1.3. Consumables

200-mesh carbon coated copper grids (Cat# CF200-Cu) were purchased from Electron Microscopy Sciences (Hatfield, PA). Illustra-NAP 25 columns (Cat# 17085201) were purchased from GE healthcare (Pittsburg, PA). 96-well white flat bottom polystyrene microplates (Cat# 3912) were purchased from Corning (Corning, NY). P2 size exclusion gel (Cat# 1504118) was purchased from Bio-Rad (Hercules, CA). LightCycler 480 Multiwell Plate 96 qPCR plates (white) (Cat# 04729692001) were purchased from Roche (Penzberg, Upper Bavaria, Germany). Amicon Ultra-0.5 mL centrifugal filters (30,000 NMWL) (Cat# UFC503024) were purchased from EMD Millipore (Burlington, MA).

2. Equipment

The major equipment that was used in this study includes: H-7500 transmission electron microscope (TEM) (Hitachi), Nanodrop 2000 UV-Vis Spectrophotometer (Thermo Scientific), Barnstead nanopure water purifying system (Thermo Fisher), SB3D1020 3D Nutation Mixer orbital shaker (Southwest Science), ultrasonic cleaner bath sonicator (Cat# 97043-968) (VWR), 5424 R centrifuge (Eppendorf), Synergy H1 plate reader (Biotek), Dual-Fl-UV-800 fluorometer (Horiba) with cuvette (105-251-15-40) (Hellma Analytics), high-performance liquid chromatography 1100 (Agilent) with AdvanceBio Oligonucleotide C18 column (653950-702, 4.6 x 150 mm, 2.7 µm) (Agilent), Matrix-assisted laser desorption/ionization time-of-flight mass spectrometer (MALDI-TOF-MS) (Voyager STR), LightCycler 96 qPCR instrument (Roche), and Amersham Typhoon gel imager (GE Healthcare).

3. Methods

Modeling. Statistics of association of oligos to SNAs with patterned or randomly distributed complements with varying segment number (*n*) were calculated using a mean-field lattice kinetic model, based on the Langmuir adsorption isotherm. Binding is assumed to take place through the initial binding of a single segment to an unoccupied complement site, at a rate proportional to the bulk solution oligo concentration c_{bulk} ([Target]), followed by sequential binding of adjacent segments (if an unoccupied complementary neighbor site exists) at a rate proportional to some higher effective local concentration c_{eff}. Desorption of a lone single segment or of a bound segment on either end of a sequence of bound segments is treated using the same rate constant; desorption from the interior of a sequence of bound segments is assumed negligible.

For a patterned heteroMV SNA, with *n* segments each templated sequence of *n* segments is assumed to equilibrate with the bath of oligos independently, as if all templates were on parallel tracks with no crossover possibility. Oligos are assumed to bind a track in a contiguous series of segments; the possibility of unbound internal loops is neglected. The fraction of tracks having an oligo bound at all segments from *i* to *j* with $i \le j \le n$ is designated f_{ij}, leading to ½ $n \times (n+1)$ distinct binding arrangements to track. To express the rates of all possible adsorption and desorption events, it is useful to define individual site occupancies,

$$\Theta_i = \sum_{i' \le i, j' \ge i} f_{i'j'}$$

as well as the occupancies by lower and upper border segments,

$$\Theta_{i,low} = \sum_{j' \ge i} f_{ij'} \; ; \Theta_{j,up} = \sum_{i' \le j} f_{i'j}$$

(For *i,j* out of the range from 1 to *n* we can define $\Theta_i, \Theta_{i,low}, \Theta_{j,up} = 1$.)

Equations for the rates of the elementary processes then become:

Rates for binding the first and subsequent segments depend on the bulk or effective concentration and the fractional occupations of the complementary sites. The rate of the elementary process of adsorption at a single segment *i* follows the Langmuir model:

$$r_{on,i} = k_{on} c_{bulk} (1 - \Theta_i)$$

The rates of binding of segments with higher or lower indices depend on the effective concentration and the probability that the adjacent site will be occupied. Noting that the complementary site at the next higher segment may either be free, with probability $1 - \Theta_{j+1}$, or occupied by the lowest bound segment of a different oligo, with probability $\Theta_{j+1,low}$, the fraction of bound oligos that have a free site at *j*+1 is incorporated into the elementary step rate as:

$$r_{i,j \to i,j+1} = k_{on} c_{eff} f_{i,j} \frac{\left(1 - \Theta_{j+1}\right)}{\left(1 - \Theta_{j+1} + \Theta_{j+1,low}\right)}.$$

Similarly,

$$r_{i,j\to i-1,j} = k_{on} c_{eff} f_{i,j} \frac{(1-\Theta_{i-1})}{(1-\Theta_{i-1}+\Theta_{i-1,up})}.$$

The rates of full desorption of oligos bound at a single segment *i*, or of lowering the valency by 1 segment at the lower or upper end, all have the same simple form:

$$r_{off,i} = k_{off} f_{ii}$$

$$r_{i,j\to i+1,j} = k_{off} f_{i,j}$$

$$r_{i,j\to i,j-1} = k_{off} f_{i,j}$$

From these elementary steps, master equations for all occupancies f_{ij} can be written and were integrated numerically to give kinetics of binding assuming constant and well-mixed c_{bulk}.

Random heteroMV SNAs with *n* segments were treated in an analogous manner, with the introduction of a distribution of track lengths created through this random deposition. Again, we neglect the possibility of crossover across tracks, assuming that the addition of a new path will be cancelled out by the disruption of another path. To determine this distribution, we define a nearest neighbor number *m*, which represents how many sites are within range of a bound site. Assuming random distribution of oligos, the probability that *no* sites within range will have the correct sequence to bind one of *n* total segments is

$$x = \left(\frac{n-1}{n}\right)^m$$

This expression gives the fraction of all sites with a track length of 1. The probability that the track will end in each successive step is $\left(\frac{n-1}{n}\right)^{m-1}$, as the "backward" option is eliminated. The mean-field probability of finding a track corresponding to each *i*,*j* starting and ending segment is calculated using this approach; in the end, only the length *n*'= *j*-*i*+1 is used. Kinetic trajectories for each subset of tracks of length *n*' are calculated in parallel exactly as for templated systems, and the results are weighted according to the number of tracks of different length.

For both types of systems, the kinetic trajectories were calculated at fixed c_{bulk} ([Target]) until converged at an equilibrium. The results at equilibrium depend on the following parameters in dimensionless units: c_{bulk}, K_d (individual segment binding affinity, equal to k_{off}/k_{on}), c_{eff}, and *m*. For the data in Figure 1d, c_{bulk} was held constant at a value of 0.01 while K_d was varied with values of 1, 0.1, and 0.01. For Figure 1e, K_d was held constant at a value of 1 while c_{bulk} was varied with values of 0.0001, 0.01, and 1. For Figure 1f, both parameters were held constant with c_{bulk} = 0.01 and K_d = 1. Finally, all modeling results presented herein were generated with c_{eff} = 10 and *m* = 6. The mean valency was calculated as:

$$valency = \frac{\sum_{i,j}(i-j+1)f_{ij}}{\sum_{i,j} f_{ij}}$$

It was assumed that each bound site had six nearest neighbors (*m* = 6) based on the hexagonal packing of Au atoms on the nanoparticle surface.[1]

Synthesis of gold nanoparticles. The synthesis protocol was adapted from a published protocol from Mirkin and colleagues.[2] Briefly, the glassware was cleaned with aqua regia (HNO3 + 3HCl) and washed with nanopure water at least 5 times. Then, 250 ml of 1 mM gold (III) chloride trihydrate solution was transferred into a 500 ml round-bottom flask coupled to a reflux condenser (water flowing through the condenser). Next, the solution was heated and rigorously stirred till the refluxing rate reached ~1 drip/s. While the gold solution was refluxing, 25 ml of 38.8 mM sodium citrate tribasic dihydrate solution was rapidly injected into the flask (one injection within 1 sec). The flask was resealed. The solution was kept stirring and turned to clear, to black, and then to wine-red. 15 mins after adding citrate solution, the heat was removed to allow the reaction to cool to room temperature (usually takes 2-4 hours). Lastly, the cool AuNP solution was filtered through a 0.45 μm acetate filter and stored at 4°C. The concentration of the AuNPs were determined by UV-Vis by measuring the absorbance at 520 nm with the Nanodrop instrument. The size of AuNPs was characterized by transmission electron microscopy (TEM). TEM measurements were acquired on a Hitachi H-7500 transmission electron microscope at an accelerating voltage of 80 kV in the Robert P. Apkarian Integrated Electron Microscopy Core at Emory University. Briefly, 5 μl of gold solution was deposited on a 200-mesh carbon coated copper grid (Electron Microscopy Sciences) for 10 mins. Excess liquid was then wicked away and AuNPs were imaged without further negative staining using the TEM.

Random heteroMV SNA synthesis. Thiolated segment strands were treated with 0.1 M DTT in disulfide cleavage buffer (170 mM phosphate buffer, pH = 8.0) for 2-3 hours at room temperature to reduce the disulfide protecting group to thiol. For heteroMV SNAs with *n* unique segments, the concentration of each segment in the mixture incubated with DTT is equal to total [DNA]/*n*. These reduced segment strands were purified using a NAP 25 size exclusion column. The oligo concentration was determined by UV-Vis. Then, ~3 μM (final concentration) thiolated oligonucleotides were mixed with ~7 nM AuNPs (final concentration) in nanopure water and incubated on an orbital shaker overnight in the dark at room temperature. Next, phosphate adjustment buffer (100 mM phosphate buffer, pH = 7.0) and SDS (10% w/v in nanopure water) were added to make a DNA-AuNP mixture with 10 mM phosphate and 0.1% w/v SDS. This mixture was incubated on an orbital shaker for another 30 min at RT. Salting buffer (10 mM phosphate buffer and 2 M NaCl, pH 7.0) was then added in eight increments, increasing total NaCl concentration stepwise as follows: 0.05, 0.1, 0.2, 0.3, 0.4, 0.5, 0.6, and 0.7 M. After each addition, the SNAs were sonicated in a bath sonicator 20–30 s and incubated on an orbital shaker for 20 min. Following salt aging to 0.7 M NaCl final concentration, SNAs were left overnight on an orbital shaker and then stored in 0.7 M NaCl at 4°C until use.

Determining number of oligos/AuNP. Salted particles (random SNAs and patterned SNAs) were washed three times by centrifugation at 13,000 rpm for 20 min at 22°C. After each spin, particles were resuspended in nanopure water. The particles were then diluted to a concentration of 0.2, 0.4, 0.6, and 0.8 nM to yield a 320 μL solution in 1x TE buffer using a stock of 20x TE Buffer (0.2 M Tris-HCl and 20 mM EDTA, pH = 7.5) and nanopure water. To dissolve the gold core and release the oligonucleotides, the particles were incubated in 10 mM KCN (using a 200 mM KCN stock buffered in KOH) for 30 min. From each sample, 100 μL was added to three wells of a 96 well plate and incubated with 100 μL of 1x Oligreen reagent for ~5 min before measuring fluorescence using the Biotek plate reader. To generate a standard curve of fluorescence vs. [DNA], 320 μL of 0, 0.1, 0.2, 0.5, 1, 1.5, and 2 ng/μL samples of unreduced DNA (mixture of same segments as the particles being measured) were first prepared in 1x TE buffer. DNA was then

incubated with 10 mM KCN for 30 min to remain consistency with particle samples. From each sample, 100 μL was added to three wells of a 96 well plate and incubated with 100 μL of 1x Oligreen reagent for ~5 min before measuring fluorescence using the plate reader. Using the standard curve, the concentration of DNA in particle samples was determined and then divided by initial AuNP concentration to determine the number of oligos per AuNP.

Melting curve measurement for random heteroMV SNAs. Salted random heteroMV SNA particles were washed three times by centrifugation at 13,000 rpm for 20 min at 22°C. After the first two spins, particles were resuspended in nanopure water. After the third spin, particles were resuspended in 1x PBS or 0.1x SSC, 0.2% Tween20 and concentrated to ~4 nM. Particles were then incubated for 1 hour with 100 nM of FAM-labeled target strand at room temperature with shaking. Following template strand hybridization, particles were washed three times at 13,000 rpm for 20 min to remove any unbound target. After the first two spins, particles were resuspended in 1x SSC and after the third spin, particles were resuspended in 4x SSC, 0.2% Tween20. A melting curve was obtained by heating the particles from 25°C to 80°C and measuring the fluorescence every 5°C using the Horiba fluorometer. Melting curves were fit on GraphPad Prism using the function: log(agonist) vs. response – variable slope equation. This fit provided a T_m for each melting curve. Normalized melting curves were obtained by plugging each data point x into the equation: (maximum fluorescence – x)/(maximum fluorescence – minimum fluorescence). The first derivative plot of each fitted curve was also plotted and fit to a gaussian distribution and the standard deviation was multiplied by 2.355 to obtain the full width at half-maximum value (fwhm). The fluorescence intensity at 80°C was used as the maximum fluorescence intensity value after melting. To determine how many targets bound to each SNA, a calibration curve was generated by measuring fluorescence intensity at 80°C of FAM-labeled target at a range of concentrations (0.1-80 nM) incubated with 4 nM T10-conjugated SNAs to control for AuNP quenching effects. T10-conjugated SNAs were prepared by adding 3 nmol of Thiol-T10 DNA to 1 mL of 10 nM AuNP, incubating at -30°C for > 2 hours, and then thawing and washing 3x in nanopure water.[3] The calibration curve was then used to convert maximum fluorescence intensity values after melting to concentration of target. Concentration of target values were then divided by 4 nM (SNA concentration) to determine targets bound per SNA.

Cy5 conjugation to target strands. Excess NHS-Cy5 (250 μg) was dissolved in 10 μL of fresh DMSO and then added to 10 nmol of amine-labeled target strands in 1x PBS with 0.1 M $NaHCO_3$. The reaction was left for > 4 hs at room temperature. After incubation, unreacted NHS-Cy5 and salts were removed by P2 gel filtration and purified using an analytical-scale reverse-phase HPLC with an Agilent AdvanceBio Oligonucleotide C18 column. Product was eluted in Solvents A: 0.1 M TEAA and B: ACN with a linear gradient of 10-100% Solvent B over 45 min at 0.5 mL/min flow rate. The desired product was characterized by MALDI-TOF-MS. 3-HPA was dissolved in 50% ACN/H2O containing 0.1% TFA and 5 mg/mL ammonium citrate as matrix to acquire MALDI-TOF-MS spectra. The concentration of the strands was determined by UV-Vis using a Nanodrop instrument.

van't Hoff binding affinity measurement. Salted particles were centrifuged three times at 13,000 rpm for 20 min and after each centrifugation the supernatant was removed and replaced with fresh nanopure water. In a qPCR plate, 20 μL solutions of SNAs and Cy5-labeled targets at a 1:1, 5:1, or 10:1 target:SNA ratio were prepared in 1x SSC, 0.2% Tween20 buffer. The targets were labeled with Cy5 rather than FAM due to its enhanced brightness allowing for more sensitive fluorescence detection. The total concentration of SNA and Cy5-targets (C_T) was varied, while

maintaining a 1:1, 5:1, or 10:1 target:SNA ratio, to prepare a series of C_T values from 3.5 to 30, 10.5 to 90, or 19.25 to 165 nM, respectively. Samples were left to hybridize at RT for one hour to hybridize before measurement of T_m. Using the qPCR instrument (LightCycler 96), the plate was incubated at 40°C for 5 min before heating to 65°C at a rate of 2.4°C/minute with 25 fluorescent measurements obtained per °C. Melting curves were fit using the GraphPad Prism log(agonist) vs. response- variable slope function, providing a T_m for each melting curve. Triplicate T_m values for each sample at each C_T value were obtained. Based on equation 1, $\ln(C_T)$ vs. $1/T_m$ was then plotted and fit to a linear curve with slope equal to R/ΔH and *y*-intercept equal to (ΔS-R*ln(4))/(ΔH). A value of 1.986 x 10^{-3} kcal K^{-1} mol^{-1} was used for R.

$$Equation\ 1:\ \frac{1}{T_m} = \frac{R}{\Delta H}\ lnC_T + \frac{\Delta S - R\ ln4}{\Delta H}$$

From the values of ΔH and ΔS, values for ΔG and K_{eq} were obtained using equation 2 and equation 3, respectively, and extrapolating data to 298 K.

$$Equation\ 2: \Delta G = \Delta H - T\Delta S$$

$$Equation\ 3: K_{eq} = e^{-\Delta G/RT}$$

Native PAGE. Segment strands (120 μM each) were annealed to template strand (100 μM) in 0.1x PBS, 0.1x Phosphate Adjustment Buffer (10 mM phosphate buffer). For the purified complex in lane 9, hybridized DNA was then incubated with 100x TCEP for ~30 min to remove thiol protecting groups. Hybridized DNA was then purified with a 30k amicon filter by centrifuging 3x at 14,000 rcf for 30 min, removing flow-through (containing non-hybridized segments, excess TCEP, and thiol protecting group), and adding ~500 μL of 1x SSC to the concentrated sample after each centrifugation. 10 pmol of segments 1-6 mixture (lane 1) and 5 pmol of template (lane 2) or annealed complex (lanes 3-9) in 1x TBE with 1x DNA loading dye were added to a 6% native PAGE gel and run for an hour at 60 V. Gels were stained with 1x SYBR Gold reagent for 10 min and imaged on the Amersham Typhoon gel imager.

Patterned and mispatterned SNA synthesis. Non-reduced thiolated segment strands (120 μM each) were annealed to the template strand (100 μM) in 0.1x PBS, 0.1x Phosphate Adjustment Buffer (10 mM phosphate buffer). Hybridized DNA was then incubated with 100x TCEP for ~30 min to remove thiol protecting groups. Hybridized and reduced DNA was then purified with a 30k amicon filter by centrifuging 3x at 14,000 rcf for 30 min, removing flow-through (containing non-hybridized segments, excess TCEP, and thiol protecting group), and adding ~500 μL of 1x SSC to the concentrated sample after each centrifugation. 500 nM (final concentration) of annealed DNA was then added to ~10 nM AuNPs suspended in 10 mM phosphate buffer with 0.1% w/v SDS and 10 mM NaCl to maintain DNA hybridization and shook on an orbital shaker for one hour at room temperature. Particles were then salt-aged to 0.7 M NaCl as described above and backfilled with ~3 μM thiol-T10 DNA (final concentration) 20 min after the last salt addition to ensure complete saturation of the AuNP surface with DNA. Particles were left overnight on an orbital shaker at room temperature and then stored at 4°C until ready for use.

Determining number of templates/patterned SNA. Salted particles were centrifuged three times at 13,000 rpm for 20 min and after each centrifugation the supernatant was removed. After the first two spins, particles were resuspended in 1x SSC (pre-dehybridization measurement) or nanopure water (post-dehybridization measurement). After the third spin, particles were

resuspended in 4x SSC, 0.2% Tween20 and concentrated to ~4 nM. Particles were then heated from 25°C to 80°C and the fluorescence was measured every 5°C using the fluorometer. The maximum fluorescence intensity value was then converted to templates bound per SNA using the calibration curve and method presented above.

Melting curve measurement for patterned SNAs. Salted particles (patterned and mispatterned SNAs) were washed three times by centrifugation at 13,000 rpm for 20 min at 22°C. After the first two spins, particles were resuspended in nanopure water. After the third spin, particles were resuspended in 1x PBS and concentrated to ~4 nM. Particles were then incubated for 1 hour with 100 nM of FAM-labeled no-spacer target strand at room temperature with shaking. Following template strand hybridization, particles were washed three times at 13,000 rpm for 20 min to remove any unbound target. After the first two spins, particles were resuspended in 0.1x SSC, 0.2% Tween20 and after the third spin, particles were resuspended in 4x SSC, 0.2% Tween20. Using the qPCR instrument (Light cycler 96), the plate was incubated at 40°C for 5 min before heating to 71°C at a rate of 2.4°C/minute with 25 fluorescent measurements obtained per °C. Melting curves were fit using the GraphPad Prism log(agonist) vs. response- variable slope function, providing a T_m for each melting curve. The first derivative plot of each fitted curve was also plotted and fit to a gaussian distribution and the standard deviation was multiplied by 2.355 to obtain the full width at half-maximum value (fwhm). To determine how many targets bound to each SNA, a calibration curve was generated by measuring fluorescence intensity at 80°C of FAM-labeled target at a range of concentrations (0.1-80 nM) incubated with 4 nM T10-conjugated SNAs to control for AuNP quenching effects. T10-conjugated SNAs were prepared by adding 3 nmol of Thiol-T10 DNA to 1 mL of 10 nM AuNP, incubating at -30°C for > 2 hours, and then thawing and washing 3x in nanopure water.[3] The calibration curve was then used to convert maximum fluorescence intensity values after melting to concentration of target. Concentration of target values were then divided by 4 nM (SNA concentration) to determine targets bound per SNA.

Figure S1. Modeling the impact of target concentration and surface occupancy on mean binding valency.

(a-b) Modeling results predicting the mean binding valency of random *n*=1-6 SNAs as the target concentration (a) and the fraction of binding sites on the surface bound to a target (b) increases, assuming the K_d of each individual segment binding to the particle equals 1. (c-d) Modeling results predicting the mean binding valency of random *n*=1-6 SNAs as the target concentration (c) and the fraction of binding sites on the surface bound to a target (d) increases, assuming the K_d of each individual segment binding to the particle equals 0.01. The target concentrations and K_d values used for these modeling results are of arbitrary units (a.u.).

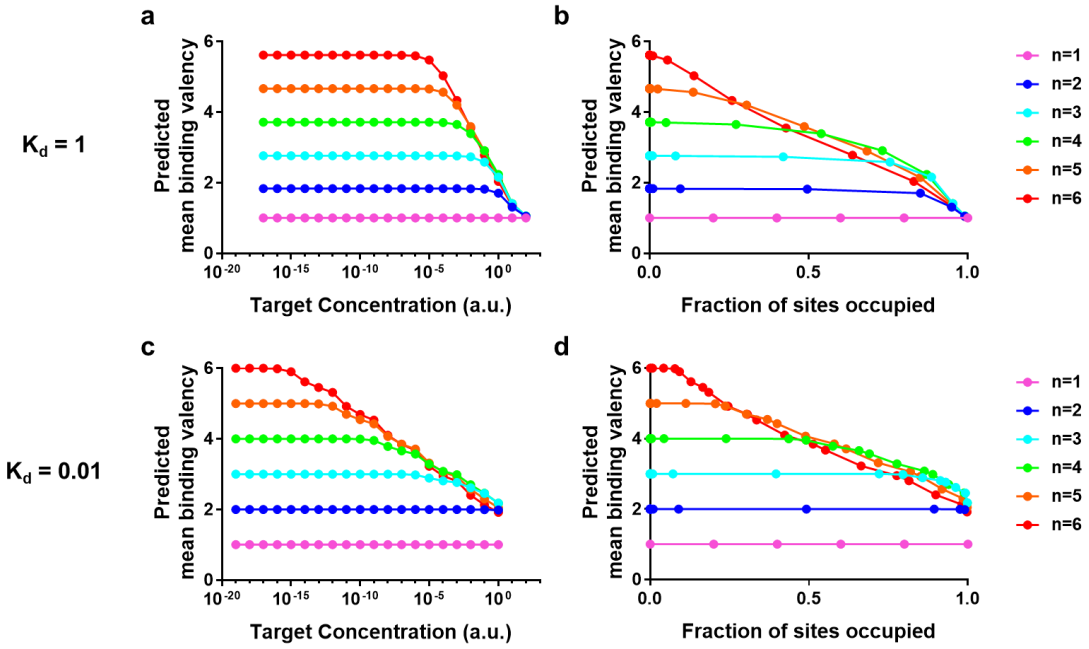

Figure S2. Depiction of multivalent DNA binding interaction.
(a) Table showing binding sequences for segments 1-6 as well as the spacer-containing (underlined) target and the template/target with no spacers. The melting temperature was determined using the nearest neighbor thermodynamic estimate on the *OligoAnalyzer* software package available on IDT's website. For predicted T_m's, the following conditions were used: oligonucleotide concentration = 250 nM, Na^+ = 150 mM, and Mg^{2+} = 0 mM. (b) Schematic depicting the binding interaction between segments 1-6 with the target and with the template/no-spacer target. Based on data not shown, adenine bases in the spacer region of the spacer-containing target are depicted hybridizing the thymine bases at the 3' end of the T10 linker, resulting in the likely formation of a 1 nt gap between segments 2 and 3 and between segments 4 and 5 and a single-strand nick between segments 3 and 4. Alternatively, the no-spacer target/template forms a single-strand nick between each binding interaction.

a

Name	Sequence (5' to 3')	T_m (°C)
segment 1	ACTCTACCACATATA	37
segment 2	TCCTTGGGAACC	41
segment 3	GACAGTAAATGCG	38.4
segment 4	CAGCAAATGCCA	40.3
segment 5	AGGTCATGAATATAA	35
segment 6	ACAGCAAATATCCT	38.5
target	AGGATATTTGCTGTCTTTATATTCATGACCT ACTGGCATTTGCTGAACGCATTTACTGTC ACGGTTCCCAAGGACCTATATGTGGTAGAGT	-
template/ target- no spacers	AGGATATTTGCTGTTTATATTCATGACCT TGGCATTTGCTGCGCATTTACTGTC GGTTCCCAAGGATATATGTGGTAGAGT	79

b

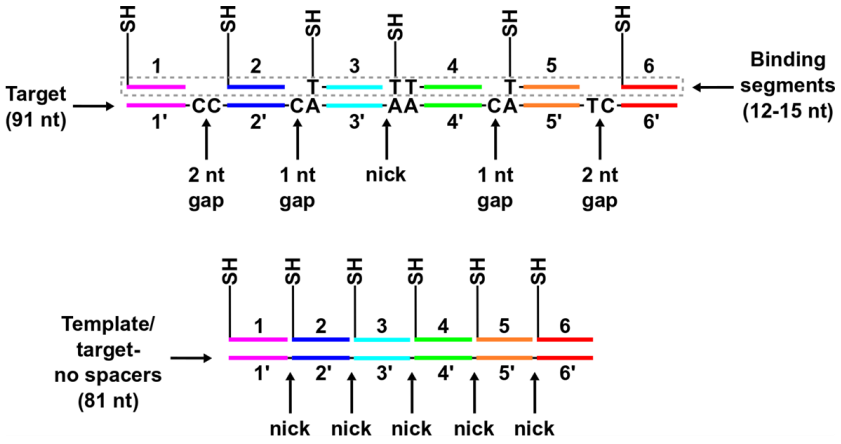

Figure S3. Synthesis and characterization of heteroMV SNAs.
(a) Representative TEM image of citrate stabilized AuNPs used in this work. (b) Histogram plotting the particle diameter based on analysis of 326 AuNPs imaged using TEM. (c) Schematic showing synthesis of heteroMV SNAs. Equimolar concentrations of thiolated-T10-segments 1-6 were added to 13 nM AuNPs and then salt-aged to yield heteroMV SNAs with *n* unique oligos ($n \leq 6$). (d) Schematic illustrating the protocol for determining the number of oligos per AuNP. HeteroMV SNAs were incubated with 10 mM KCN for 30 min to dissolve the AuNP core. Released oligos were then incubated with Quant-iT OliGreen reagent for ~5 min before measuring fluorescence. (e) Calibration curves for *n*=1 and *n*=6 SNAs were generated by incubating a range of concentrations of segments 1 or segments 1-6 (for *n*=1 and *n*=6 SNAs, respectively) with Quant-iT OliGreen reagent (mean ± SEM). Each data point represents the mean value of triplicate fluorescence values for each sample at each concentration. Each curve was linearly fit to obtain a conversion factor between fluorescence intensity and [DNA]. (f) Plots showing the DNA density (DNA/AuNP) for *n*=1 and *n*=6 SNAs (mean ± SEM). Each data point represents the mean value from 4 samples prepared at 0.2, 0.4, 0.6, and 0.8 nM initial AuNP concentration, with triplicate fluorescence values for each sample at each concentration. An unpaired student *t* test showed no statistical difference (P > 0.05) for DNA/AuNP between *n*=1 and *n*=6 SNAs.

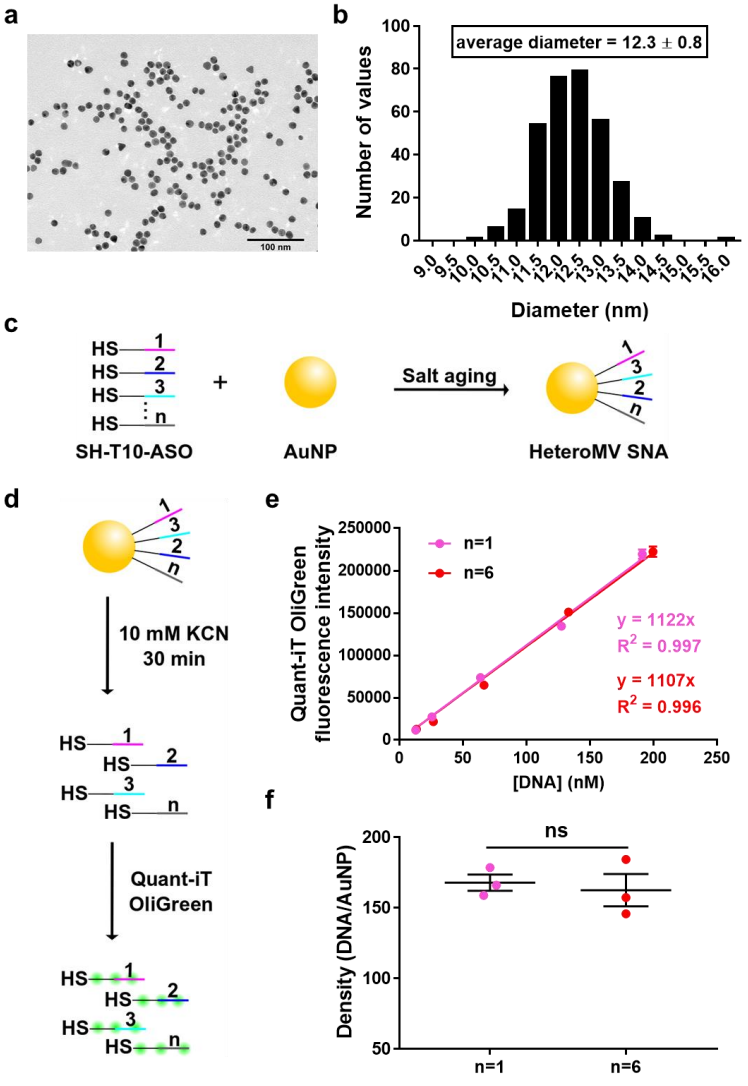

Figure S4. Raw melts and binding capacity determination for random heteroMV SNAs. (a-b) Raw melting curves for *n*=1-6 SNAs after hybridizing in (a) 1x PBS or (b) 0.1x SSC, 0.2% Tween20. (c-d) Normalized melting curves for *n*=1-6 SNAs after hybridizing in (c) 1x PBS or (d) 0.1x SSC, 0.2% Tween20. Each data point represents the mean and SEM of triplicate measurements. (e) Scheme showing how to calculate number of targets bound per AuNP from fluorescence intensity value after melting using a calibration curve. (f) Calibration curve generated by measuring fluorescence intensity at 80°C of target at different concentrations incubated with T10 AuNPs. (g-h) The impact of increasing *n* on targets bound per SNA after hybridizing target to SNA in 1x PBS (g) or in 0.1x SSC, 0.2% Tween20 (h). Error bars represent standard error of the mean. Values were compared using unpaired student *t* tests (*P < 0.05; **P < 0.01; ***P < 0.001).

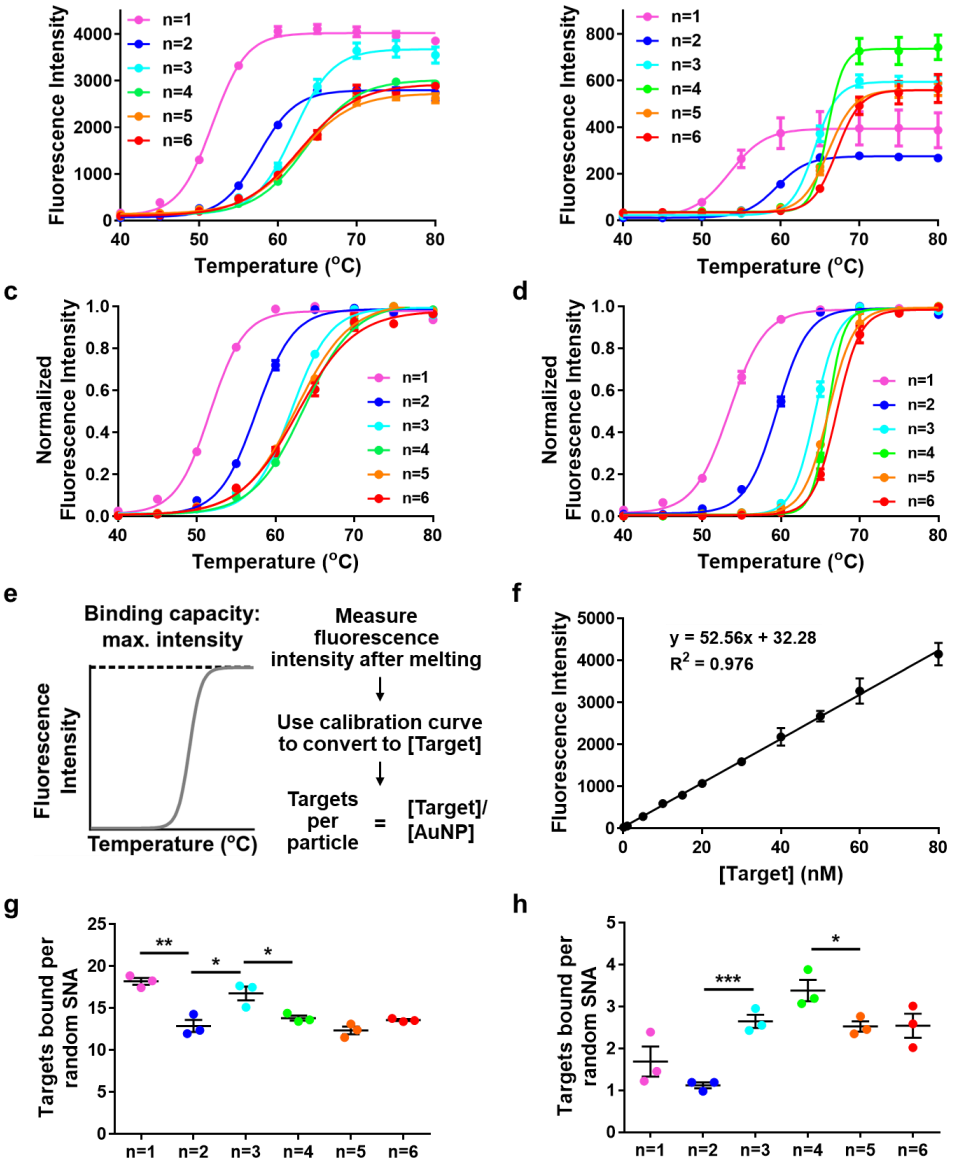

Figure S5. Characterization of modified oligonucleotides.
(a) Structure of oligonucleotide modifications used in the current work. (b-c) HPLC traces and MALDI-TOF-MS of the (b) no-spacer Cy5-labeled target and the (c) Cy5-labeled target after reacting the corresponding amine targets with NHS-Cy5. Arrows represent the material collected from HPLC. (d) Table of calculated masses, measured m/z values found, and percent error of starting materials and Cy5-labeled products.

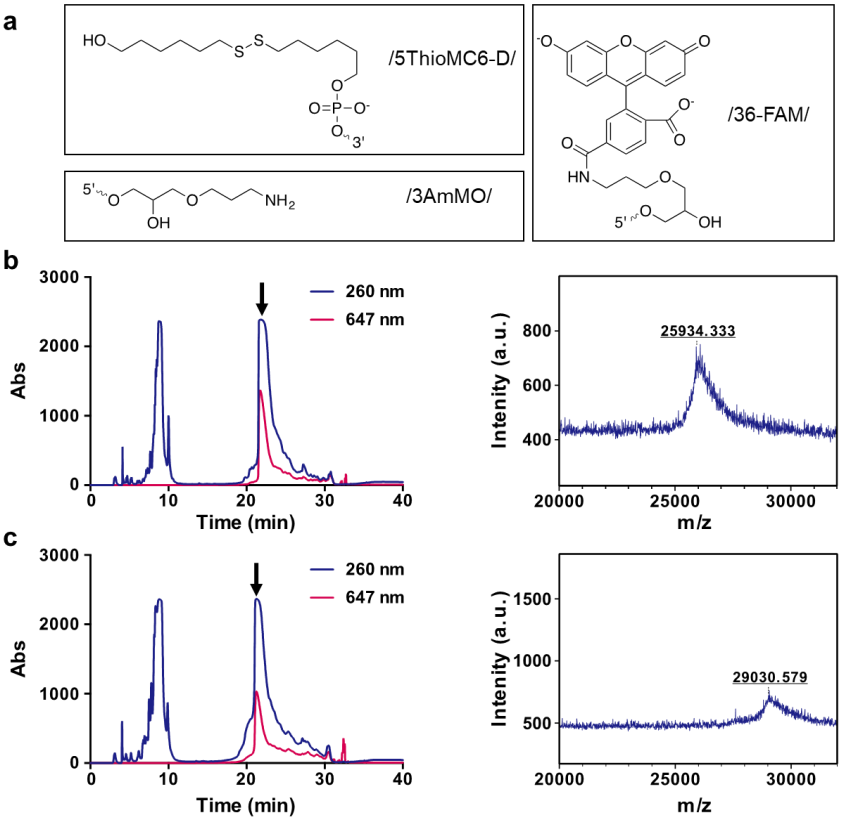

d

Sample	Calculated mass (Da)	m/z found (Da)	%Error
amine target-no spacers	25247.4	25503.8	1.02
Cy5 target-no spacers	25714.1	25934.3	0.86
amine target	28250.3	28770.4	1.84
Cy5 target	28717.0	29030.6	1.09

Figure S6. Impact of target:SNA ratio on random heteroMV SNAs binding thermodynamics. (a-b) T_m (a) and fwhm (b) values in triplicate of 5 nM random *n*=1-6 SNAs incubated with Cy5-labeled target at 1:1, 5:1, or 10:1 target:SNA ratios. (c-e) ΔH (c), -TΔS (d), and log(K_{eq}) (e) values for *n*=1-6 random SNAs incubated with Cy5-labeled target at 1:1, 5:1, or 10:1 target:SNA ratios. Data represents mean values of three replicates and error bars correspond to SEM. The complete set of T_m values from which ΔH and -TΔS were calculated are shown in Table S1 for the 1:1 target:SNA ratio data and Table S4 for the 5:1 and 10:1 target:SNA ratio data. ΔH and -TΔS values are shown in Table S2 for the 1:1 target:SNA ratio data and Table S5 for the 5:1 and 10:1 target:SNA ratio data. Finally, log(k_{eq}) values are shown in Table S3 for the 1:1 target:SNA ratio data and Table S5 for the 5:1 and 10:1 target:SNA ratio data.

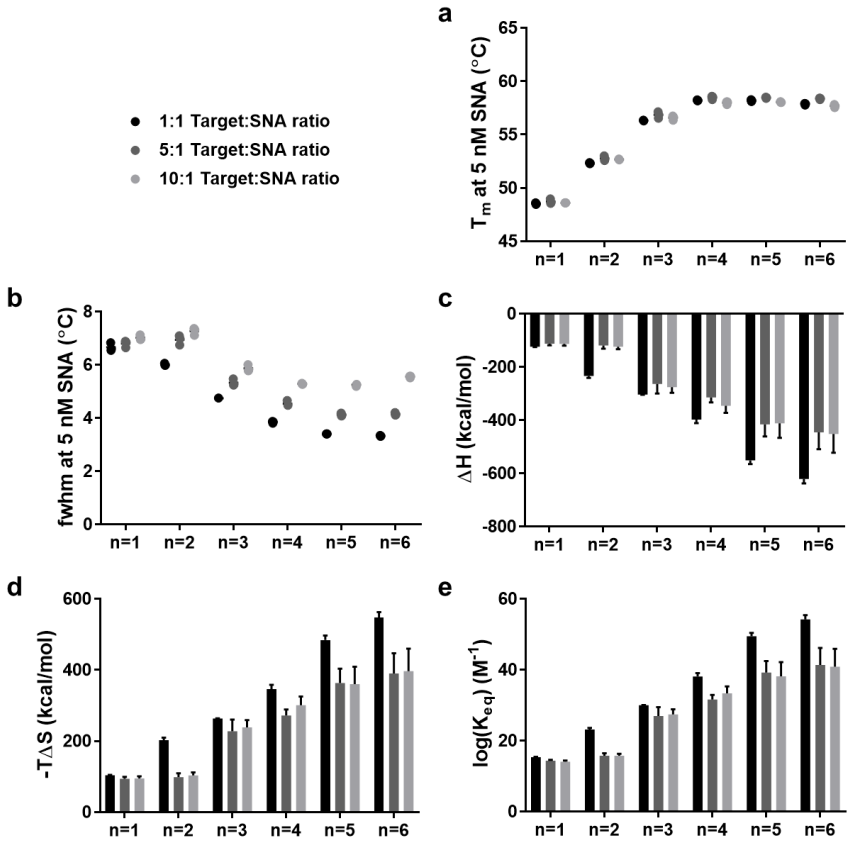

Figure S7. Preparation of template/segments complex and PAGE characterization.
(a) Schematic showing preparation of template/segments complex. Unreduced T10-segments 1-6 were first annealed to the template at 1.2:1 ratio (120 μM of segment 1, 120 μM of segment 2, etc. and 100 μM of template). Following hybridization, thiol protecting groups on segments 1-6 were cleaved using 100x TCEP for ~30 min. Finally, template/segments complex was purified using a 30k amicon filter to remove unbound segments 1-6, thiol protecting group, and TCEP. (b) 6% native PAGE gel showing binding of segments 1-6 to the template. Lane 1: segments 1-6 mixture, Lane 2: template, Lane 3: annealed segment 1-template complex, Lane 4: annealed segments 1-2-template complex, Lane 5: annealed segments 1-3-template complex, Lane 6: annealed segments 1-4-template complex, Lane 7: annealed segments 1-5-template complex, Lane 8: annealed segments 1-6-template complex, Lane 9: annealed, reduced, and purified segments 1-6-template complex. With the addition of each segment to the template, the duplex's mobility through the gel was further retarded.

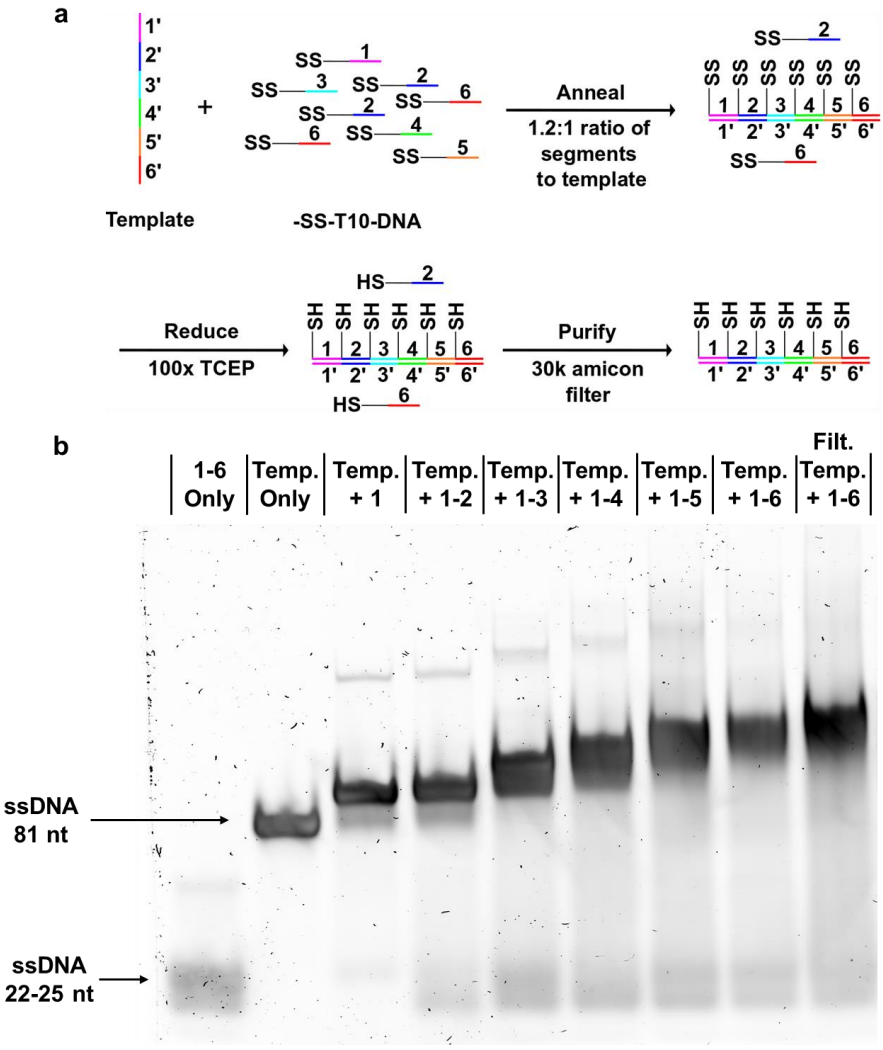

Figure S8. Geometric model of template/segments complex attached to surface of AuNP. 2D geometric model (drawn to scale) of the hybridized template/segments 1-6 complex attached to the surface of a 13 nm gold nanoparticle. The AuNP has a radius of ~6.5 nm and a circumference of ~40.8 nm. When assuming the T10 spacer on segments 1-6 adds an additional 6.3 nm between particle surface and complex lying tangential to surface, the particle and T10 has a radius of 12.8 nm (80.4 nm circumference).[4] If we assume the template/segments complex is ~27.5 nm long (length of 81mer duplex), then we can calculate that the complex will wrap around 34% of the particle surface. Moreover, since segments 1-6 are not connected, there will be "single stranded nicks" that will allow the complex to accommodate for the local curvature of the gold nanoparticle.

AuNP radius ~ 6.5 nm
circumference of AuNP ~ 40.8 nm
T10 length ~ 6.3 nm
circumference of AuNP + T10 ~ 80.4 nm
total 81mer duplex length ~ 27.5 nm

Complex wraps around ~ 34% of particle circumference

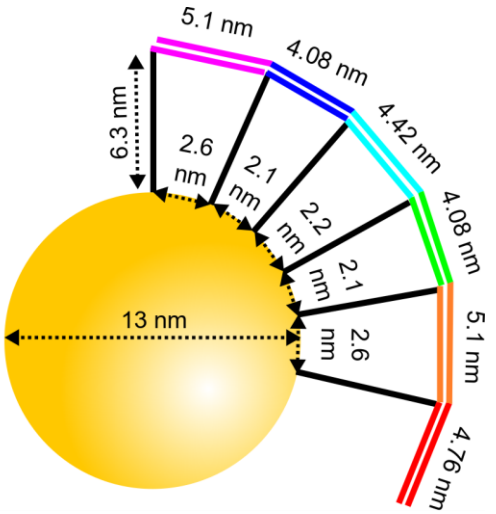

Figure S9. Scheme, raw melts, and characterization for patterned SNAs template melting. (a) Schematic for thermal melting assay for determining templates bound to patterned SNAs before and after dehybridization of the template. Salted patterned SNAs were either washed 3x with 1x SSC (pre-dehybridization) or 3x with nanopure water (post-dehybridization) (mean ± SEM from three triplicate melting curves). (b) Raw melting curves for patterned SNAs pre-dehybridization and post-dehybridization. (c) Table of T_m values, fwhm values, and number of targets bound from melting curves in (b) (mean ± SEM).

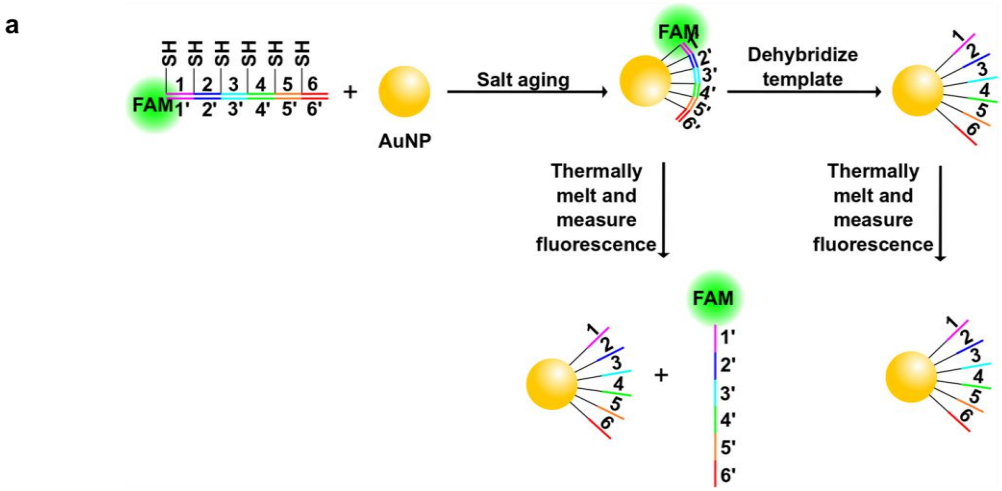

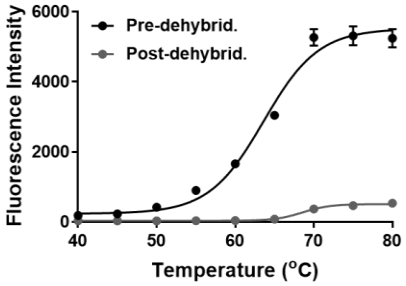

c

Target	Pre-dehbrid.	Post-dehybrid.
T_m (°C)	63.6 ± 0.4	68.5 ± 0.2
fwhm	13.0 ± 0.1	6.6 ± 0.3
Targets bound	24.8 ± 1.3	2.4 ± 0.1

Figure S10. Preparation of mispatterned SNAs and determination of segment densities for patterned and mispatterned SNAs.

(a) Schematic for synthesis of *n*=6 mispatterned SNAs. Segments 1-6 were hybridized to the shuffled mispatterned template before incubation with particle. Particle was then salt-aged and washed with water to dehybridize mispatterned template, yielding mispatterned heteroMV SNA. (b) Table including patterned and mispatterned template sequences. The melting temperature was determined using the nearest neighbor thermodynamic estimate on the *OligoAnalyzer* software package available on IDT's website. For predicted T_m's, the following conditions were used: oligonucleotide concentration = 250 nM, Na^+ = 150 mM, and Mg^{2+} = 0 mM. (c) Plots showing the DNA density (DNA/AuNP) for *n*=6 patterned and mispatterned SNAs (mean ± SEM). Each data point represents the mean value from 4 samples prepared at 0.2, 0.4, 0.6, and 0.8 nM initial AuNP concentration, with triplicate fluorescence values for each sample at each concentration. An unpaired student *t* test showed no statistical difference (P > 0.05) for the number of DNA/AuNP between patterned and mispatterned SNAs.

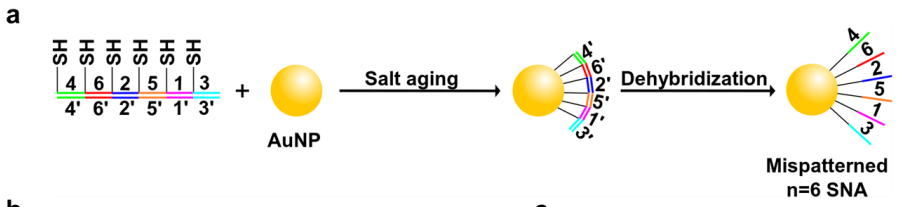

b

Name	Sequence (5' to 3')	T_m (°C)
Patterned template	AGGATATTTGCTGTTTATATT CATGACCTTGGCATTTGCTG CGCATTTACTGTCGGTTCCC AAGGATATATGTGGTAGAGT	79
Mispatterned template	TGGCATTTGCTGAGGATATT TGCTGTGGTTCCCAAGGATT ATATTCATGACCTTATATGTG GTAGAGTCGCATTTACTGTC	78.3

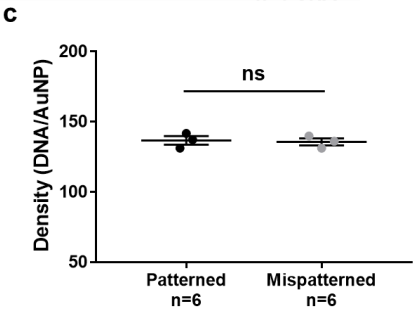

Figure S11. Melting characterization of patterned SNAs binding excess targets.
(a) Triplicate raw melting curves for patterned and mispatterned *n*=6 SNAs after hybridizing to the no-spacer target at a 25:1 target:SNA ratio in 1x PBS and washing with 0.1x SSC, 0.2% Tween20 buffer. Each data point represents a single fluorescence reading. (b-c) Melting temperature (T_m) (b) and full width at half-maximum (fwhm) (c) values (mean ± SEM) for patterned and mispatterned SNAs after fitting data raw data in (a). Values were compared using an unpaired student *t* test ($^{ns}P > 0.05$; $^{**}P < 0.01$). The larger fwhm value for patterned SNAs suggests patterned SNAs bind some targets with higher valencies that are less achievable for mispatterned SNAs, while both particle types form lower valency interactions as well due to the high target concentration that saturates the surface, resulting in a broader melting transition. (d) Calibration curve generated by measuring fluorescence intensity at 80°C of target at different concentrations incubated with T10 AuNPs.

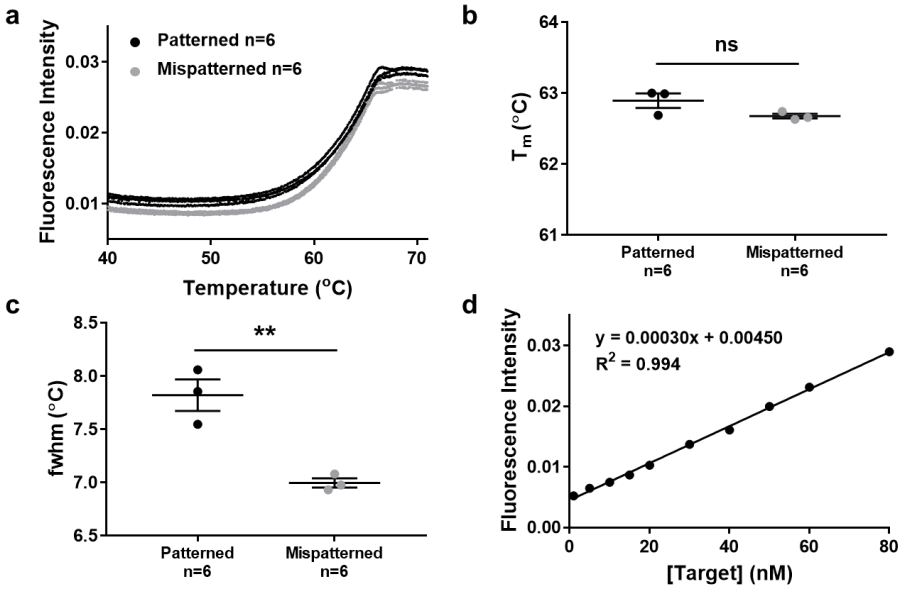

Figure S12. Raw melts, ΔH, and -TΔS values for patterned, random and mispatterned *n*=6 heteroMV SNAs.

(a) Triplicate raw thermal melting curves for patterned, random, and mispatterned *n*=6 SNAs binding the no-spacer Cy5-labeled target. For melting curves shown: [SNA] = 3.5 nM, [target] = 3.5 nM, C_T = 7 nM. Each melting curve was fit as described in the methods section and a T_m for each curve was calculated. (b-c) ΔH (b) and -TΔS (c) values for patterned, random, and mispatterned *n*=6 SNAs binding the no-spacer Cy5-labeled target. Error bars represent mean ± SEM from three replicate measurements. T_m values for random *n*=6 SNAs are shown in Table S1 and T_m values for patterned and mispatterned SNAs are shown in Table S6.

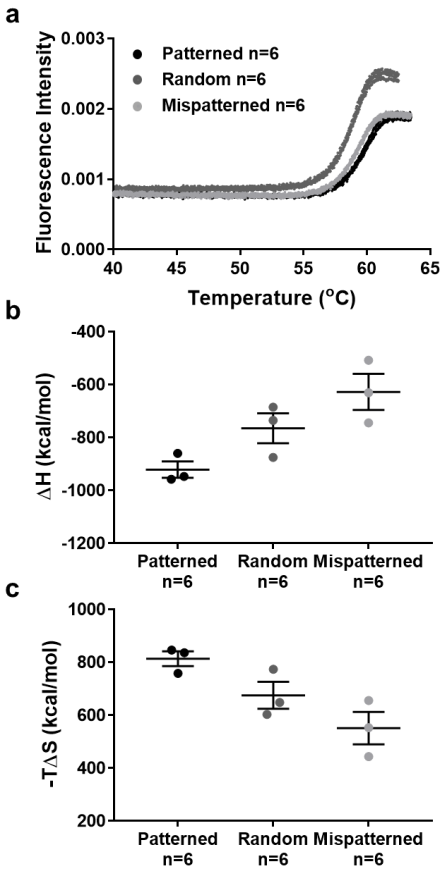

Table S1. T_m values for random heteroMV SNAs from van't Hoff melting assay.
T_m values (mean ± SEM) from three individual melting curves (3 separate hybridizations and melts) for *n*=1-6 SNAs binding to Cy5-labeled targets at a 1:1 ratio (C_T = [SNA] + [Target]). Targets were hybridized to SNAs in 1x SSC, 0.2% Tween20 buffer for 1 hour at room temperature. Thermal melting curves were obtained by reading fluorescence increase with a qPCR instrument as Cy5-target dehybridizes from SNA.

		T_m (°C)					
Target	C_T (nM)	*n*=1	*n*=2	*n*=3	*n*=4	*n*=5	*n*=6
target	3.5	46.89 ± 0.04	51.47 ± 0.04	-	-	57.91 ± 0.02	57.65 ± 0.02
	5	47.43 ± 0.00	51.75 ± 0.05	56.00 ± 0.04	57.85 ± 0.03	57.98 ± 0.03	57.72 ± 0.02
	7	47.92 ± 0.08	51.88 ± 0.01	56.16 ± 0.02	58.09 ± 0.04	58.11 ± 0.03	57.80 ± 0.02
	10	48.52 ± 0.04	52.32 ± 0.03	56.33 ± 0.02	58.21 ± 0.03	58.19 ± 0.05	57.87 ± 0.05
	15	49.25 ± 0.06	52.66 ± 0.04	56.59 ± 0.05	58.39 ± 0.03	58.35 ± 0.02	57.94 ± 0.04
	22	49.95 ± 0.06	53.07 ± 0.03	57.02 ± 0.03	58.74 ± 0.07	58.65 ± 0.02	58.28 ± 0.02
	30	50.35 ± 0.07	53.37 ± 0.03	57.24 ± 0.01	58.83 ± 0.02	58.73 ± 0.07	58.41 ± 0.03
target-no spacers	3.5	47.38 ± 0.02	52.03 ± 0.01	-	-	58.58 ± 0.03	58.45 ± 0.01
	5	47.90 ± 0.02	52.32 ± 0.06	56.51 ± 0.05	58.25 ± 0.02	58.62 ± 0.02	58.53 ± 0.00
	7	48.53 ± 0.02	52.60 ± 0.03	56.74 ± 0.03	58.42 ± 0.03	58.79 ± 0.02	58.61 ± 0.02
	10	49.09 ± 0.03	52.86 ± 0.05	56.93 ± 0.04	58.61 ± 0.07	58.90 ± 0.04	58.76 ± 0.03
	15	49.85 ± 0.01	53.22 ± 0.02	57.17 ± 0.03	58.73 ± 0.04	58.98 ± 0.01	58.78 ± 0.06
	22	50.58 ± 0.03	53.77 ± 0.04	57.51 ± 0.03	59.07 ± 0.03	59.27 ± 0.04	59.01 ± 0.10
	30	51.04 ± 0.09	54.14 ± 0.02	57.66 ± 0.05	59.20 ± 0.01	59.35 ± 0.08	59.04 ± 0.03

Table S2. Thermodynamic values for random heteroMV SNAs.
ΔH, ΔS, and ΔG values (mean ± SEM) from linear fits of three $\ln(C_T)$ vs. $1/T_m$ curves for *n*=1-6 SNAs binding to Cy5-labeled targets. $\ln(C_T)$ vs. $1/T_m$ curves were obtained from T_m values in Table S1. ΔG values were calculated using a temperature value of 298 K.

Target	Parameter	*n*=1	*n*=2	*n*=3	*n*=4	*n*=5	*n*=6
target	ΔH (kcal/mol)	-124.64 ± 1.26	-234.39 ± 7.28	-304.37 ± 0.37	-398.16 ± 13.24	-551.71 ± 13.95	-621.61 ± 16.47
	ΔS (kcal/mol*K)	-0.348 ± 0.004	-0.681 ± 0.022	-0.884 ± 0.001	-1.162 ± 0.040	-1.625 ± 0.042	-1.838 ± 0.050
	ΔG (kcal/mol)	-20.91 ± 0.08	-31.51 ± 0.63	-40.88 ± 0.05	-51.86 ± 1.34	-67.34 ± 1.34	-73.86 ± 1.64
target-no spacers	ΔH (kcal/mol)	-118.81 ± 1.58	-217.90 ± 1.07	-333.47 ± 5.94	-412.38 ± 16.42	-584.19 ± 24.58	-765.03 ± 56.78
	ΔS (kcal/mol*K)	-0.329 ± 0.005	-0.629 ± 0.003	-0.971 ± 0.018	-1.204 ± 0.049	-1.720 ± 0.074	-2.266 ± 0.171
	ΔG (kcal/mol)	-20.67 ± 0.11	-30.50 ± 0.09	-44.18 ± 0.56	-53.72 ± 1.71	-71.64 ± 2.50	-89.84 ± 5.70

Table S3. Affinity values for random heteroMV SNAs.

log(K_{eq}) (mean ± SEM) from triplicate ΔG values (Table S2) and β values (β = $K_{eq}^{multi\ (n>1)}/K_{eq}^{mono\ (n=1)}$) for *n*=1-6 SNAs binding to Cy5-labeled targets.

Target	Parameter	*n*=1	*n*=2	*n*=3	*n*=4	*n*=5	*n*=6
target	log(K_{eq}) (M^{-1})	15.35 ± 0.06	23.12 ± 0.46	30.00 ± 0.04	38.06 ± 0.98	49.41 ± 0.98	54.20 ± 1.20
	β		6.0×10^{7}	4.5×10^{14}	5.1×10^{22}	1.2×10^{34}	7.1×10^{38}
target-no spacers	log(K_{eq}) (M^{-1})	15.17 ± 0.08	22.38 ± 0.07	32.42 ± 0.41	39.42 ± 1.25	52.57 ± 1.83	65.92 ± 4.18
	β		1.6×10^{7}	1.8×10^{17}	1.8×10^{24}	2.5×10^{37}	5.7×10^{50}

Table S4. T_m values for random heteroMV SNAs from 5:1 and 10:1 target:SNA ratio van't Hoff melting assays.

T_m values (mean ± SEM) from three individual melting curves (3 separate hybridizations and melts) for *n*=1-6 SNAs binding to the Cy5-labeled target at a 5:1 or 10:1 target:SNA ratio (C_T = [SNA] + [Target]). Targets were hybridized to SNAs in 1x SSC, 0.2% Tween20 buffer for 1 hour at room temperature. Thermal melting curves were obtained by reading fluorescence increase with a qPCR instrument as Cy5-target dehybridizes from SNA.

		T_m (°C)					
Target:SNA ratio	**C_T (nM)**	***n*=1**	***n*=2**	***n*=3**	***n*=4**	***n*=5**	***n*=6**
5:1	**10.5**	47.07 ± 0.07	51.57 ± 0.03	56.06 ± 0.09	57.83 ± 0.10	57.95 ± 0.12	57.96 ± 0.21
	15	47.51 ± 0.14	51.88 ± 0.08	56.29 ± 0.13	58.07 ± 0.12	58.26 ± 0.11	58.07 ± 0.11
	21	48.15 ± 0.09	52.23 ± 0.09	56.57 ± 0.09	58.29 ± 0.14	58.31 ± 0.08	58.21 ± 0.15
	30	48.73 ± 0.12	52.77 ± 0.12	56.85 ± 0.18	58.48 ± 0.09	58.46 ± 0.03	58.37 ± 0.04
	45	49.55 ± 0.18	53.62 ± 0.19	57.19 ± 0.24	58.77 ± 0.18	58.76 ± 0.14	58.54 ± 0.13
	66	50.13 ± 0.21	54.37 ± 0.22	57.46 ± 0.24	59.03 ± 0.12	58.85 ± 0.14	58.69 ± 0.15
	90	50.86 ± 0.12	55.27 ± 0.25	57.85 ± 0.22	59.32 ± 0.11	59.18 ± 0.14	59.08 ± 0.08
10:1	**19.25**	46.91 ± 0.08	51.28 ± 0.06	55.82 ± 0.09	57.42 ± 0.11	57.36 ± 0.06	57.18 ± 0.09
	27.5	47.45 ± 0.04	51.60 ± 0.03	56.00 ± 0.12	57.64 ± 0.10	57.68 ± 0.16	57.42 ± 0.11
	38.5	48.08 ± 0.05	52.14 ± 0.07	56.31 ± 0.13	57.95 ± 0.12	57.81 ± 0.07	57.60 ± 0.16
	55	48.60 ± 0.00	52.67 ± 0.02	56.58 ± 0.11	57.99 ± 0.09	58.05 ± 0.02	57.68 ± 0.08
	82.5	49.36 ± 0.05	53.54 ± 0.05	56.85 ± 0.16	58.36 ± 0.11	58.30 ± 0.16	57.91 ± 0.19
	121	49.94 ± 0.04	53.99 ± 0.03	57.15 ± 0.20	58.58 ± 0.19	58.26 ± 0.09	57.99 ± 0.15
	165	50.75 ± 0.04	54.77 ± 0.13	57.47 ± 0.08	58.77 ± 0.05	58.59 ± 0.12	58.33 ± 0.09

Table S5. Thermodynamic and affinity values for random heteroMV SNAs from 5:1 and 10:1 target:SNA ratio assays.

ΔH, ΔS, and ΔG values (mean ± SEM) from linear fits of three $\ln(C_T)$ vs. $1/T_m$ curves for *n*=1-6 SNAs binding to the Cy5-labeled target at a 5:1 or 10:1 target:SNA ratio. $\ln(C_T)$ vs. $1/T_m$ curves were obtained from T_m values in Table S4. ΔG values were calculated using a temperature value of 298 K. $\log(K_{eq})$ (mean ± SEM) from triplicate ΔG values and β values ($\beta = K_{eq}^{multi\ (n>1)}/K_{eq}^{mono\ (n=1)}$) for *n*=1-6 SNAs binding to the Cy5-labeled target.

Target:SNA ratio	Parameter	*n*=1	*n*=2	*n*=3	*n*=4	*n*=5	*n*=6
5:1	ΔH (kcal/mol)	-113.15 ± 5.87	-119.47 ± 12.12	-264.35 ± 36.02	-315.06 ± 18.37	-416.53 ± 44.87	-446.39 ± 63.49
	ΔS (kcal/mol*K)	-0.314 ± 0.018	-0.329 ± 0.037	-0.764 ± 0.110	-0.913 ± 0.056	-1.219 ± 0.136	-1.309 ± 0.191
	ΔG (kcal/mol)	-19.51 ± 0.38	-21.41 ± 0.98	-36.70 ± 3.37	-43.06 ± 1.76	-53.37 ± 4.46	-56.30 ± 6.53
	$\log(K_{eq})$ (M^{-1})	14.31 ± 0.28	15.71 ± 0.72	26.93 ± 2.47	31.59 ± 1.29	39.16 ± 3.27	41.31 ± 4.79
	β		2.49×10^{1}	4.14×10^{12}	1.91×10^{17}	7.10×10^{24}	9.99×10^{26}
10:1	ΔH (kcal/mol)	-113.67 ± 6.54	-124.51 ± 9.28	-276.25 ± 21.66	-346.01 ± 27.07	-412.28 ± 54.48	-452.66 ± 70.32
	ΔS (kcal/mol*K)	-0.317 ± 0.020	-0.346 ± 0.029	-0.802 ± 0.066	-1.009 ± 0.082	-1.209 ± 0.165	-1.332 ± 0.213
	ΔG (kcal/mol)	-19.14 ± 0.47	-21.40 ± 0.78	-37.29 ± 2.01	-45.43 ± 2.63	-51.99 ± 5.42	-55.66 ± 6.86
	$\log(K_{eq})$ (M^{-1})	14.05 ± 0.35	15.70 ± 0.57	27.36 ± 1.48	33.33 ± 1.93	38.15 ± 3.98	40.84 ± 5.03
	β		4.54×10^{1}	2.06×10^{13}	1.94×10^{19}	1.26×10^{24}	6.24×10^{26}

Table S6. T_m values for patterned SNAs from van't Hoff melting assay.
T_m values (mean ± SEM) from three individual melting curves (3 separate hybridizations and melts) for *n*=6 patterned and mispatterned SNAs binding to Cy5-labeled targets at 1:1 ratio (C_T = [SNA] + [target]). Targets were hybridized to SNAs in 1x SSC, 0.2% Tween20 buffer for 1 hour at room temperature. Thermal melting curves were obtained in the same buffer solution by reading fluorescence increase with a qPCR instrument as Cy5-target dehybridizes from SNA.

		T_m (°C)	
Target	C_T (nM)	patterned	mispatterned
target-no spacers	3.5	59.50 ± 0.07	58.89 ± 0.04
	5	59.38 ± 0.06	58.94 ± 0.07
	7	59.59 ± 0.04	59.04 ± 0.02
	10	59.52 ± 0.07	59.11 ± 0.05
	15	59.65 ± 0.03	59.22 ± 0.02
	22	59.89 ± 0.09	59.55 ± 0.04
	30	59.94 ± 0.05	59.63 ± 0.06
target	3.5	58.92 ± 0.03	58.67 ± 0.03
	5	58.88 ± 0.04	58.66 ± 0.02
	7	59.01 ± 0.04	58.85 ± 0.06
	10	59.01 ± 0.02	58.88 ± 0.06
	15	59.08 ± 0.04	59.03 ± 0.01
	22	59.38 ± 0.06	59.38 ± 0.03
	30	59.64 ± 0.05	59.63 ± 0.06

Table S7. Thermodynamic and affinity values for patterned SNAs.
ΔH, ΔS, ΔG, log(K_{eq}), and β ($K_{eq}^{multi\ (n>1)}/K_{eq}^{mono\ (n=1)}$) values (mean ± SEM) from linear fits of three ln(C_T) vs. 1/T_m curves for *n*=6 patterned and mispatterned SNAs binding to Cy5-labeled targets. ln(C_T) vs. 1/T_m curves were obtained from T_m values in Table S6. ΔG values were calculated using a temperature value of 298 K.

Target	Parameter	patterned	mispatterned
target-no spacers	ΔH (kcal/mol)	-921.56 ± 31.10	-627.52 ± 68.35
	ΔS (kcal/mol*K)	-2.730 ± 0.094	-1.849 ± 0.206
	ΔG (kcal/mol)	-107.99 ± 3.18	-76.54 ± 7.05
	log(K_{eq}) (M^{-1})	79.25 ± 2.33	56.16 ± 5.18
	β	1.19×10^{64}	9.88×10^{40}
target	ΔH (kcal/mol)	-688.07 ± 34.45	-495.17 ± 15.78
	ΔS (kcal/mol*K)	-2.031 ± 0.104	-1.451 ± 0.048
	ΔG (kcal/mol)	-82.73 ± 3.56	-62.63 ± 1.59
	log(K_{eq}) (M^{-1})	60.70 ± 2.61	45.96 ± 1.17
	β	2.26×10^{45}	4.04×10^{30}

Supporting References

1. Lobo Maza, F.; Grumelli, D.; Carro, P.; Vericat, C.; Kern, K.; Salvarezza, R. C., The role of the crystalline face in the ordering of 6-mercaptopurine self-assembled monolayers on gold. *Nanoscale* **2016,** *8* (39), 17231-17240.
2. Hill, H. D.; Mirkin, C. A., The bio-barcode assay for the detection of protein and nucleic acid targets using DTT-induced ligand exchange. *Nat. Protoc.* **2006,** *1* (1), 324-36.
3. Liu, B.; Liu, J., Freezing Directed Construction of Bio/Nano Interfaces: Reagentless Conjugation, Denser Spherical Nucleic Acids, and Better Nanoflares. *J. Am. Chem. Soc.* **2017,** *139* (28), 9471-9474.
4. Murphy, M. C.; Rasnik, I.; Cheng, W.; Lohman, T. M.; Ha, T., Probing single-stranded DNA conformational flexibility using fluorescence spectroscopy. *Biophys. J.* **2004,** *86* (4), 2530-7.